Ceramics International **23** (1997) 521–536
© 1997 Elsevier Science Limited and Techna S.r.l.
Printed in Great Britain. All rights reserved
PII: S0272-8842(96)00065-X
0272-8842/97 $17.00+0.00

Overall Shape of Sintered Alumina Compacts

Necati Özkan & Brian J. Briscoe

Department of Chemical Engineering and Chemical Technology, Imperial College of Science, Technology and Medicine, London SW7 2BY, UK

(Received 27 March 1996; accepted 3 June 1996)

Abstract: The extent of the thermally induced shrinkage during sintering of nominally homogeneous ceramic compacts depends upon the green density; compacts with a low green density shrink more than those with a higher density. Therefore, shape distortions of compacts with variable density during their sintering is inevitable. The overall shapes of various sintered alumina compacts, prepared using different types of alumina agglomerates, is described. The agglomerates were prepared using organic polymer [poly(vinyl alcohol) (PVA) and poly(ethylene glycol) (PEG)] binders and the influence of the particle agglomerates size and the water content in the agglomerates is considered. The extent of the shape distortions in the cylindrical sintered compacts were reduced with the application of lubricants to the die walls. The agglomerate properties are shown to affect the overall shape of the sintered compacts significantly. The compacts, produced using the wet (plastisized) agglomerates, have the smallest shape distortions. A prediction of the sintered shape evolution is obtained using a first order model. The model predicts that the shape distortions in the sintered compacts increase with the increasing of the sintered density and a good agreement between the predicted and measured data is demonstrated. © 1997 Elsevier Science Limited and Techna S.r.l.

1 INTRODUCTION

There is now a rising demand on the level of the required precision of the external dimensional tolerances, as well as internal microstructure, of advanced ceramic materials. In principle, a satisfactory final ceramic product, with the required dimensional tolerances, is obtained from a green compact with an appropriate self-similar shape and with a homogeneous density. However, by the very nature of ceramic production processing it is difficult to achieve the latter condition, particularly in the case of "dry" powder processing. When the dimensional tolerances for ceramic components, requiring close tolerances, are not met, machining of the surfaces is required. Ceramic materials are intrinsically brittle in nature, as well as being exceptionally hard. These properties make them rather difficult to machine to the final shape. The machining processes are slow, inefficient and very expensive, and may also introduce defects into the samples and produce a deterioration in their mechanical properties. In addition, it will often be impossible to machine complex shaped products. For these reasons, the characterisation and optimisation of the overall shape of sintered ceramic parts is a very important element in ceramic manufacture.

This paper seeks to show that by optimising the processing and materials parameters, the overall shape of the final product can be controlled to an acceptable precision for the alumina compacts prepared by the uniaxial die-pressing technique. These compacts possess a non-uniform green density due to the creation of an uneven stress distribution within the sample, which is controlled in the major part by the wall boundary conditions between the compact and the die.[1–5] In this paper,

the effects of the green density variations, upon the sintering (shrinkage) kinetics, are investigated in order to explain the shape distortions in the sintered compacts, produced using cylindrical green compacts with an inhomogeneous density distribution. The effects of the aspect ratio, the state of the wall lubrication and the agglomerate properties (binder type, binder content and moisture level) on the overall fully sintered shape of die-pressed cylindrical alumina compacts as determined experimentally are described.[1–3] The evolution of the shapes of the sintered compacts are analysed and predicted using first order predictive models. Model experiments, which suggest a route for the manufacturing of the near net shape cylindrical compacts, are also reported. In addition to the simple cylindrical compacts, the variation of the overall shape of alumina tubes, prepared by the uniaxial dry die-pressing technique, are also reported and discussed.

2 EXPERIMENTAL PROCEDURE

Different types of alumina agglomerates were used in order to produce green compacts by uniaxial die-pressing in cylindrical dies. The compacts were ~13 mm in diameter and the aspect ratio (height/diameter) ranged from 0.5 to 1.5. They were single-ended compacted using planar punches and in certain cases the die–powder interface was lubricated with zinc stearate (BDH Chemical Ltd, UK). Basically, two organic binders were used; poly(vinyl alcohol) (PVA, from BDH Chemical Ltd, UK, molecular weight = 14000) and poly(ethyl glycol) (PEG, from BDH Chemical Ltd, UK, molecular weight = 4000). The alumina powders were supplied by Morgan Matroc, UK and Sumitoma, Japan. Two agglomeration methods were used; solution agglomeration and spray drying. The resulting agglomerates were sieved using standard wire meshes and sizes in the range from 53 to 212 μm were prepared. In some cases the agglomerates were pre-conditioned in controlled humidity environments prior to the compaction. The details of the preparation of these agglomerates and green compacts are reported elsewhere.[1–3] Some of the properties of agglomerates used and the means of their preparation are given Table 1.

The sequential stages of the binder removal and the sintering of these green compacts were carried out in a tubular furnace (Carbolite, UK) with a programmable temperature controller. The actual temperature of the furnace environment was measured using a calibrated thermocouple (R type thermocouple, Carbolite, UK), which was situated adjacent to the sample. For the binder removal stage, the compacts were heated to 500°C with a heating rate of 2°C/min and maintained at this temperature for 12 h to ensure sufficient removal of the binders from the system. After the binder removal step, the compacts were then heated to the isothermal sintering temperatures with a heating rate of 10°C/min. The compacts were then sintered isothermally, at various temperatures, for fixed times.

Table 1. The properties of the alumina agglomerates

Agglomerate ID[a]	Agglomerate size (μm)[b]	Binder type, content (wt%)[c]	Moisture level (%H_2O)[d]	Preparation technique
A/4/V/D	53–212	PVA, 4.70	Dry (0.0)	Solution
A/4/V/W	53–212	PVA, 4.70	Wet (1.2)	Solution
A/4/V/H	53–212	PVA, 4.70	Humid (0.35)	Solution
A/4/G/D	53–212	PEG, 4.70	Dry (0.0)	Solution
A/4/G/W	53–212	PEG, 4.70	Wet (1.3)	Solution
A/2/V/D	53–212	PVA, 2.40	Dry (0.0)	Solution
A/2/V/W	53–212	PVA, 2.40	Wet (1.2)	Solution
A/2/V/H	53–212	PVA, 2.40	Humid (0.3)	Solution
A/2/G/D	53–212	PEG, 2.40	Dry (0.0)	Solution
A/2/G/W	53–212	PEG, 2.40	Wet (1.1)	Solution
A/2/G/H	53–212	PEG, 2.40	Humid (0.3)	Solution
A/2.5/V/SD	53–212	PVA, 2.45	—	Spray dry
M/4/G/SD	~100	PEG, 4.10	—	Spray dry
M/4.5/G/SD	~100	PEG, 4.75	—	Spray dry

[a]Agglomerate identification: agglomerates prepared using AKP-30 alumina (Sumitoma Ltd, Japan) with the mean particle size of 0.4 μm denoted "A" and the agglomerates prepared using M×3 alumina (Morgan Matroc, UK) with the mean particle size of 1.2 μm denoted "M".
[b]The size range of agglomerates.
[c]PVA: poly(vinyl alcohol); PEG: poly(ethylene glycol).
[d]The "dry" agglomerates were prepared by drying at 80°C in vacuum; the agglomerates with residual water which was not evaporated completely during the agglomerate preparation are designated as "wet"; and the dry agglomerates which were conditioned in a water vapour environment (saturated Na_2SO_3 solution) are designated as "humid".

The mean relative density and the mean relative open porosity of the sintered porous ceramic compacts, were obtained from the measurements of: (i) The net dry weight (W_1); (ii) the net weight after the sintered compact was saturated with distilled water (W_2); and (iii) the weight when the sintered compact was suspended, on a fine wire, in the distilled water (W_3).[6] The relative density of the sintered compacts, ρ_{sc}, was then calculated by using the following formula:

$$\rho_{sc} = \frac{W_1 \rho_w}{W_2 - W_3} + M_{wire} \quad (1)$$

where ρ is the sintered density of the compact, ρ_w is the density of water and M_{wire} is the mass of the suspension wire. The open porosity (%) was then calculated as:

$$\text{Open porosity (\%)} = \frac{W_2 - W_1}{\rho_w W_1 \left(\frac{1}{\rho_{sc}} - \frac{1}{\rho_{th}}\right)} (100) \quad (2)$$

where ρ_{th} is the theoretical density of the sintered compact (3980 kg/m^3).

The grain sizes of the sintered samples were measured from micrographs of the fractured and/or polished and thermally etched surfaces of samples using the linear intercept technique. For each measurement more than 150 grains were characterised.

The overall shape of the sintered compacts was measured by using a conventional digital micrometer with point contact anvils. The sintered compacts were placed on a vertical positioning stage, and the diameter of the sintered compact was measured as a function of the height of the compact. In order to measure the diameter of the sintered compact at a given height of the compact, the micrometer jaws were initially set to a low value, and subsequently increased to a new value. At each value of the micrometer opening, the sample was pushed through the openings of the micrometer and this procedure was repeated until the sample just passed through the openings of the micrometer. The average value between the penultimate and the last value was taken as the diameter value of the compact at a given height. The average resolution was $\sim 1\ \mu$m.

3 EXPERIMENTAL RESULTS AND DISCUSSION

3.1 Sintering and microstructural development

3.1.1 Sintering anisotropy

A typical plot of the mean radial shrinkage against the corresponding mean axial shrinkage is shown in Fig. 1. The data points are on the isotropic line, or very close to this line. Thus, the sintering of the agglomerated and compacted alumina powders used in this study may be assumed to be generally isotropic in nature.

3.1.2 Effects of green density on sintering

The green density is a primary parameter affecting the sintering rate and the ultimate microstructure of these ceramic bodies. The average green density, which determines the overall amount of shrinkage required to densify a ceramic compact, is normally used to characterise a sample prior to sintering. The effects of the green density upon the sintering rate and microstructure of ceramic compacts has been studied by numerous researchers, but the results from these studies are not entirely mutually consistent.[7–11] However, it has been shown that the green density has a significant effect upon the

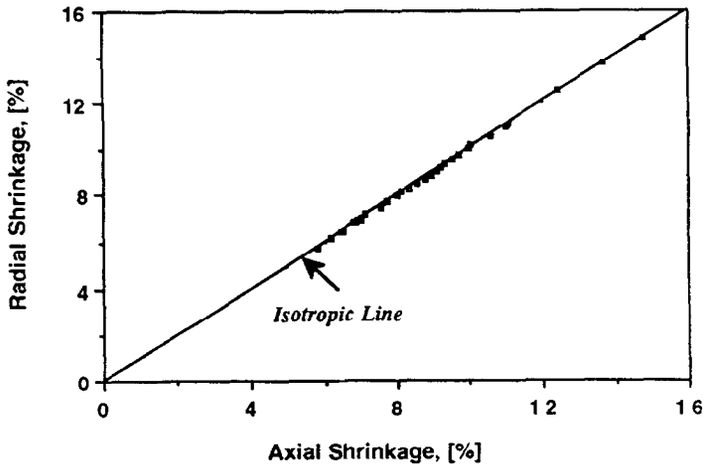

Fig. 1. Radial shrinkage vs axial shrinkage for the cylindrical alumina compacts.

sintering (shrinkage) kinetics of these types of ceramic compacts.[12] The effects of the mean green density upon the sintering behaviour of the A/2.5/V/SD and M/4.5/G/SD alumina agglomerates are briefly reported here. The isothermal sintering and shrinkage curves for the A/2.5/V/SD and M/4.5/G/SD compacts are illustrated in Figs 2 and 3, respectively. Even though the sintered density of the higher density green compacts is always higher than that of the low density green compacts, for a given time at the same temperature, the net shrinkage of the low density green compacts is always greater than that of the high density green compacts.

3.1.3 Activation energy for sintering and grain growth

The activation energy for the sintering process is taken here to be equal to the activation energy for the rate controlling diffusional mechanism, since the sintering rate is proportional to the value of the diffusion coefficient of the process which controls the sintering process. The sintering rate also depends upon the density (green and sintered) and the grain size. Therefore, a suitable general sintering rate expression should incorporate the influence of the temperature, the density and the grain size. A sufficient general sintering rate equation may be written in the following form:[13]

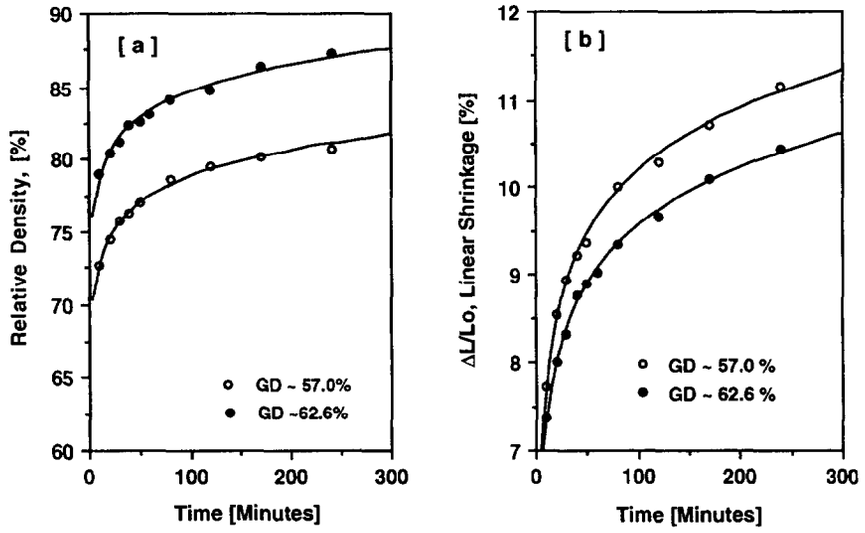

Fig. 2. (a) The isothermal sintering and (b) linear shrinkage curves for the M/4.5/G/SD alumina compacts.

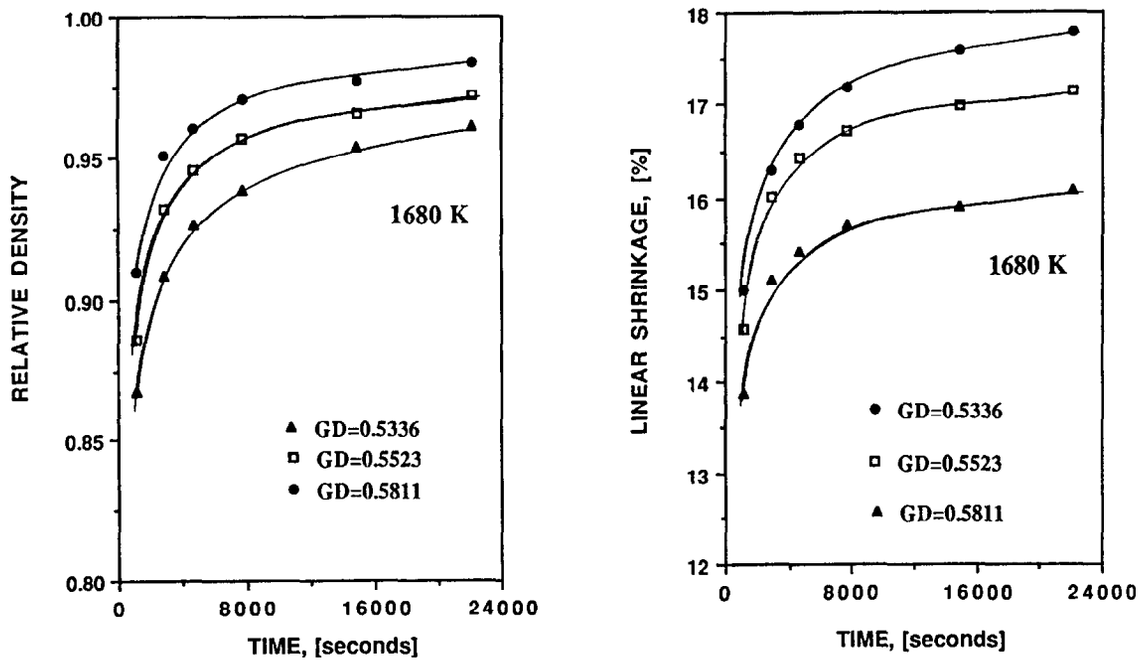

Fig. 3. (a) The isothermal sintering curves (1680 K) and (b) the isothermal shrinkage curves (1680 K) for the A/2.5/V/SD alumina compacts with initial green densities of 53.36, 55.23 and 58.11% of the theoretical density.

$$\frac{d\rho}{dt} = A \exp\left(-\frac{Q_s}{RT}\right) f(\rho) \frac{1}{G^n} \quad (3)$$

where A is a constant, Q_s is the activation energy for the sintering process, R is the gas constant, T is the absolute temperature, $f(\rho)$ is a function of the green and sintered densities, G is the grain size and n is a constant. If the sintering process is simply lattice diffusion controlled then $n=3$, and for the case of a boundary diffusion control mechanism, $n=4$. It has been shown elsewhere that the rate controlling mechanism for the sintering process in alumina is primarily that of grain boundary diffusion.[8,13]

The activation energies for the sintering and grain growth processes were estimated from the present data as 520 and 475 kJ/mol, respectively, for the A/2.5/V/SD alumina.[14] These activation energies will be used for the subsequent sintering simulations in order to predict the sintering densities of the alumina compacts with different initial green densities.

3.1.4 Open porosity and sintered density

The open porosity as a function of the sintered density for the M/4.5/G/SD compacts is illustrated in Fig. 4. Up to ~90% of the theoretical density, the pores are interconnected. The interconnected pores start to become isolated at around 90% of the theoretical density, and the pores become completely isolated at around 96% of the theoretical density. Cameron and Raj[15] have observed a change in the grain growth behaviour at approximately 90% of the theoretical density. This transition in the grain growth behaviour was related to the collapse of the pore channels to the isolated pores since the grain growth was initially limited by the mobility of the pores. The transition from the interconnected to the isolated pores may be predicted by established models which are based upon the geometry of cylindrical channels. If the grain shape is assumed to be tetrakaidecahedron, then a transition at 91% of the theoretical density is predicted,[16] which is in close agreement with the results obtained in this study.

3.1.5 Sintering simulations

The time derivative in eqn (3) was approximated by a finite difference scheme as follows:

$$\frac{d\rho}{dt} = \frac{\rho_{t+\Delta t} - \rho_t}{\Delta t} \quad (4)$$

By substituting this expression, eqn (3) becomes:

$$\rho_{t+\Delta t} = \rho_t + \left(A \exp\left(-\frac{Q_s}{RT}\right) f(\rho) \frac{1}{G^n}\right) \Delta t \quad (5)$$

For the $f(\rho)$ parameter, the following function, adopted from Swinkels and Ashby,[17] is used:

$$\frac{1}{\left(\frac{1}{1-\rho^6}\right)\left(\left(\frac{1.05\rho}{\rho_0}\right)^{0.4} - 1\right)\left(\frac{1}{\rho_0^4}\right)} \quad (6)$$

For the grain growth, the following equation was used:[14]

$$G^3 = G_0^3 + \left(k'''(\rho_0)^2 \exp\left(-\frac{Q_g}{RT}\right)\right) t \quad (7)$$

Using eqns (5) and (7), with the associated numerical values of the parameters ($A = 7.7 \times 10^{-4}$, $Q_s = 520$ kJ/mol, $n=4$, $k''' = 3.0 \times 10^{-7}$ m^3/s and

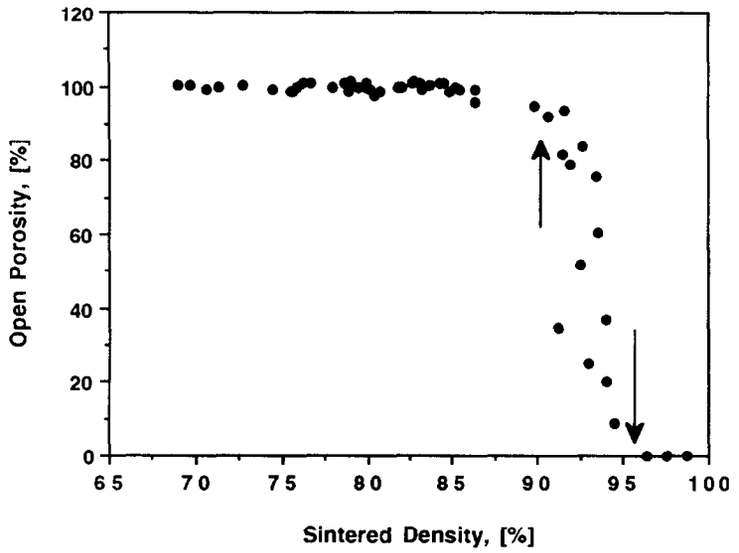

Fig. 4. The open porosity vs the sintered density for the M/4.5/G/SD alumina compacts.

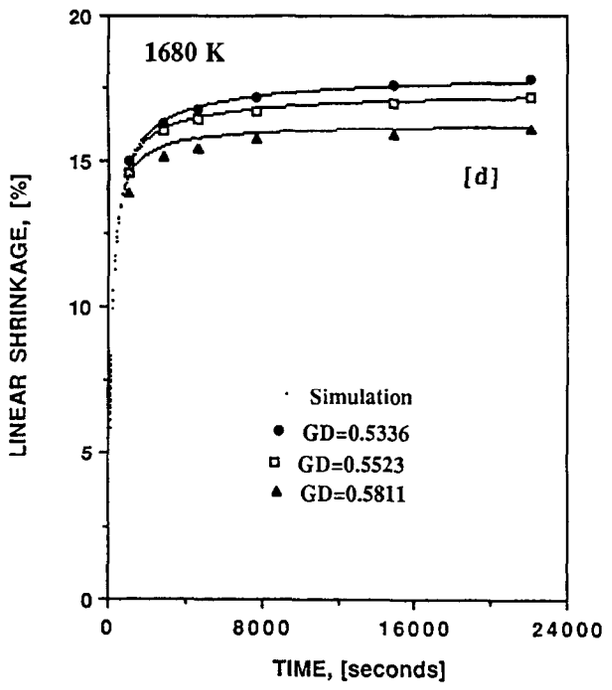

Fig. 5. The computed isothermal shrinkage curves (1680 K), together with the experimental results (the symbols represent the experimental data).

$Q_g = 475$ kJ/mol), the density–time, grain size–time and grain size–density curves were simulated.

The computed density–time and grain size–time curves, together with the experimental results for the alumina compacts, with green densities of 53.36, 55.23 and 58.11% of the theoretical density, have already been reported elsewhere.[14] The linear shrinkage–time curves can be obtained from the density–time curve, since it has been demonstrated previously that the sintering of the present alumina compacts is nearly isotropic. The linear shrinkage values were obtained using the following equation:

$$\frac{\Delta L}{L_0}[\%] = \left(1 - \left(\frac{\rho_0}{\rho_s}\right)^{\frac{1}{3}}\right) \times 100 \qquad (8)$$

The linear shrinkage–time curves for the A/2.5/V/SD compacts, sintered at 1680 K, are illustrated in Fig. 5. A good agreement between the computed and experimental results is obtained using the analytical procedure described.

The simultaneous compact densification and grain growth evolution may be described using grain size–density curves. The grain size–density curves for these compacts, with green densities of 53.36, 55.23 and 58.11% of the theoretical density, are illustrated in Fig. 6. It is clear from these curves that the grain size–density behaviour depends upon the green density; that is, the grain size of the compacts with the highest green density is the smallest at a given sintered density.

In Section 3.1.4, it has been shown that the collapse of the pore channels (interconnected pores) into the isolated pores commences at around 90% of the theoretical density. As may be seen from Fig. 6, below ~90% of the theoretical density, there is negligible grain growth. This observation agrees with the notion, introduced earlier, of the grain growth process being limited by the mobility of the pores.[15] It is reasonable to expect that long cylindrical pores will experience a greater resistance to motion than smaller spherical pores, which are isolated along the grain boundaries. Figures 4 and 6 also suggest that after the condition where the relative density, ρ, is ~96 (where all the pores become isolated), the rate of grain growth increases rapidly. The same observations were also noted by Cameron and Raj.[15]

3.2 Overall shape of sintered compacts

3.2.1 Effects of the aspect ratio upon the overall shape of the sintered alumina compacts

The effects of the sample aspect ratio upon the resulting density distribution in the alumina compacts has been reported elsewhere.[3] The extent of the density distribution increases as the aspect ratio of the sample increases. In this paper, the effects of the aspect ratio on the overall external shape of the sintered alumina compacts will be reported. In order to conveniently visualise the shape distortions in these compacts, the measured diameters of the compacts were processed by calculating dia-

Table 2. The experimental results for the A/2.5/V/SD compacts

Compact	H/D[a]	Transmission ratio[b]	G.D. (%)[c]	Diameter (μm) Max.[d]	Min.[e]	Amount of deviation (μm)[f]
A[H/D]	0.52	0.86	56.33	10789	10762	27
B[H/D]	1.01	0.68	56.18	10789	10736	53
C[H/D]	1.53	0.47	55.88	10791	10694	97

[a]The aspect ratio (H/D) = the height of the compact/the diameter of the compact).
[b]The transmission ratio = the applied pressure/the transmitted pressure.
[c]G.D(%) = the relative green density.
[d]The maximum diameter of the sintered compact.
[e]The minimum diameter of the sintered compact.
[f]The amount of deviation = the maximum diameter – the minimum diameter of the sintered compact.

meter deviation (diameter deviation = measured diameter − minimum diameter) and adding these differences to the minimum diameter value with a multiplication factor (60). These processed data were then processed, in a commercial mesh generation program, in order to depict the overall shape of the compacts. The external shape profiles of the A/2.5/V/SD alumina compacts, sintered at 1527°C for 3 h, are illustrated in Fig. 7. The results for these compacts, pressed at ~145 MPa, are summarised in Table 2.

As may be seen from Table 2, as the H/D ratio increases, the influence of the friction between the powders and the die wall increases and, as a consequence, the transmission pressure decreases. Therefore, not only will the overall density of the compacts decrease, but also the density distribution will become more non-homogeneous. The maximum gross amount of the shape deviation in the fully sintered bodies from the initial near perfect cylindrical compact geometry, expressed as absolute diametric variations, was 27, 53 and 98 μm for the compacts with aspect ratios of 0.52, 1.01 and 1.53, respectively. The corresponding transmission ratios for the corresponding green compacts were 0.86, 0.68 and 0.47, respectively.

It has already been shown that low density compacts shrink more extensively than the high density compacts. Since the transmitted pressure is always lower than the applied pressure, the compacts produced by the die-pressing route will naturally have regions with different densities. Those regions with low density will shrink more extensively than those with high density and as a result shape distortions

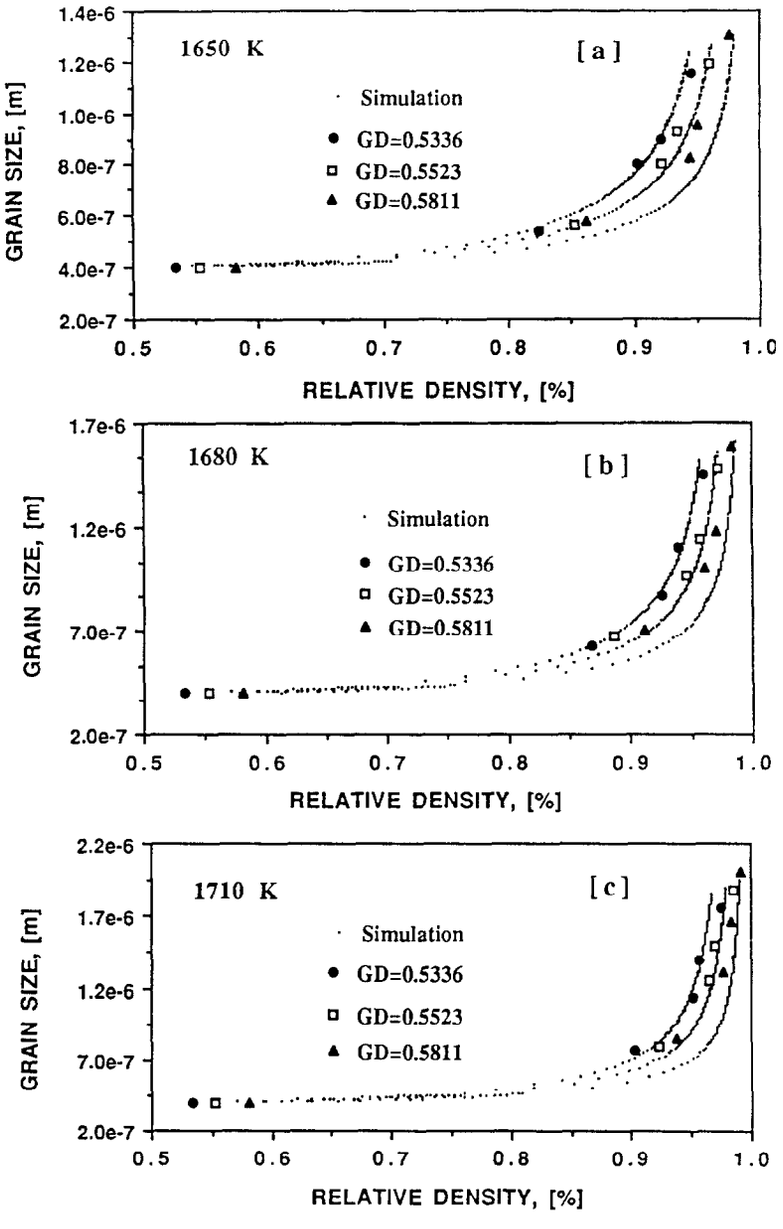

Fig. 6. The grain size against density curves for the compacts with initial green densities of 0.5336, 0.5523 and 0.5811, sintered at (a) 1650 K, (b) 1680 K and (c) 1710 K.

in the external form of the compacts are inevitable. With increasing aspect ratio the density variations will become greater and thus the shape distortions will be the most severe in those compacts with a high aspect ratio.

3.2.2 Effects of the state of wall lubrication on the overall shape of the alumina compacts

The overall shape profiles of the sintered M/4.5/G/SD compacts, prepared in the unlubricated and lubricated dies, are illustrated in Fig. 8. The results

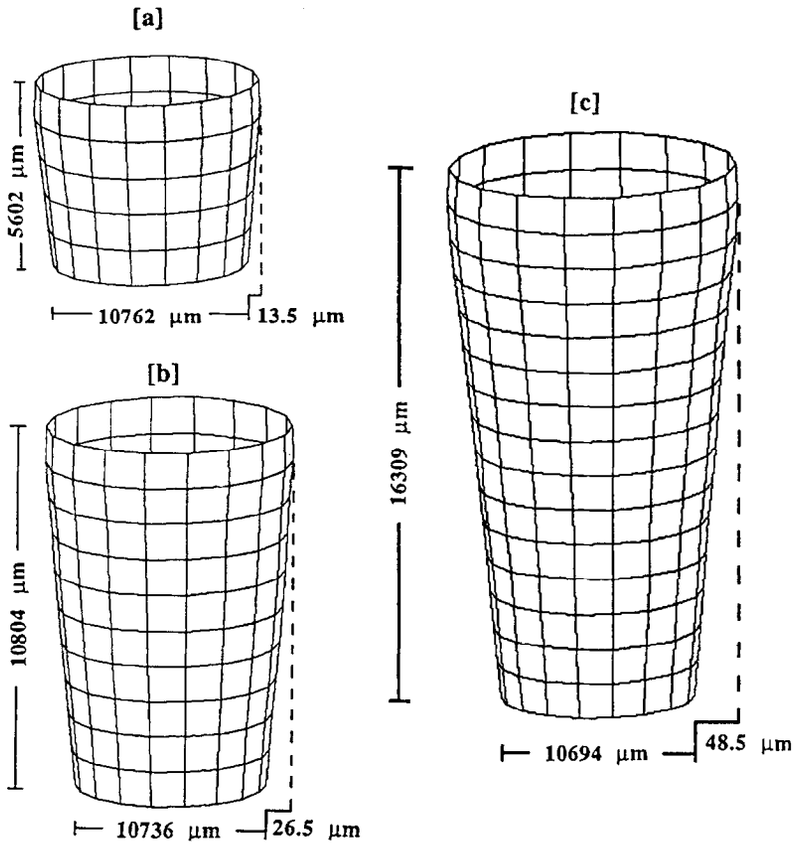

Fig. 7. The external shape profiles of the A/2.5/V/SD alumina compacts with aspect ratios of (a) 0.52, (b) 1.01 and (c) 1.53.

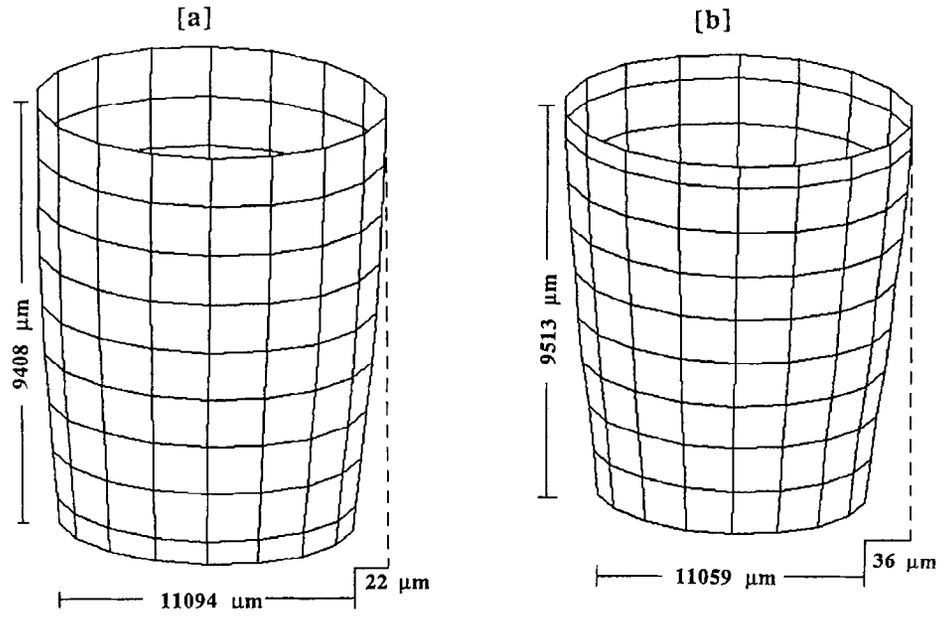

Fig. 8. The external shape profiles of the M/4.5/G/SD alumina compacts (H/D ~0.85) pressed at 222 MPa and sintered at 1582°C: (a) lubricated die; (b) unlubricated die.

Table 3. The results for the M/4.5/G/SD compacts

Compact	State of lubrication[a]	Pressure (MPa)[b]	G.D. (%)[c]	Diameter (μm) Max.[d]	Min.[e]	Amount of deviation (μm)[f]
M/4.5/G/SD (UL)	Unlubricated	222	61.05	11131	11059	72
M/4.5/G/SD (L)	Lubricated	222	61.39	11138	11094	44

[a]The lubrication state was achieved by applying the zinc stearate powder to the die walls using a brush.
[b]The ultimate compaction pressure.
[c]The relative green density at the ultimate compaction pressure.
[d]The maximum diameter of the sintered compact.
[e]The minimum diameter of the sintered compact.
[f]The amount of deviation = the maximum diameter – the minimum diameter.

for these compacts ($H/D \sim 0.85$) are summarised in Table 3.

At the compaction pressure of 222 MPa, the relative green densities of the compacts, prepared using the unlubricated and lubricated dies, are 61.05% and 61.39% of the theoretical density, respectively. The gross deviations in the geometry of the sintered bodies (represented as the difference between the maximum and minimum diameters) from the perfect self-similar cylindrical geometry are found to be 72 μm (unlubricated) and 44 μm (lubricated) for these compacts. Lubrication of the die walls with a suitable lubricant (zinc stearate) reduces the wall friction between the die wall and the compact; as a result, the transmission of the compaction pressure is more efficient. It has been shown elsewhere that the stress transmission ratio of the compacts prepared in the lubricated die is higher than that of the compacts prepared in the unlubricated die.[3] Due to the lower friction coefficient of the die wall, the compacts produced in the lubricated die possess not only an overall higher green density but also they have more homogeneous density distributions. As a consequence, the amount of gross deviation of the sintered compacts prepared in the lubricated die is lower than that of the compacts prepared in the unlubricated die.

3.2.3 Effects of the agglomerate properties (binder type, binder content, moisture level) on the overall shape of the alumina compacts

In order to investigate the effects of the agglomerate properties on the overall shape of the alumina compacts, various agglomerates with different binder type, binder content and moisture level were used to produce alumina compacts. The compacts, pressed at 370 MPa in the lubricated die, were sintered at 1527°C for 3 h. The aspect ratio of these compacts was ~ 1.07. The results for these compacts are summarised in Table 4.

It has previously been reported that adsorbed moisture (especially in the PVA system) is beneficial for the compaction of the alumina agglomerates.[1,18] The data, given in Table 4, indicate that the amount of deviation from the perfect cylindrical sintered geometry for the compacts prepared using "wet" agglomerates is significantly less than that for the compacts prepared using "dry" agglomerates. The optimal results, in terms of near net shaping, are obtained using those agglomerates prepared using PEG as a binder.

3.2.4 Evolution of the overall shape of the compacts

The prediction of the overall shape of these types of alumina compacts has previously been considered by Özkan and Briscoe.[2] In this paper, the

Table 4. The experimental results for the alumina compacts prepared using various agglomerates

Compact[a]	Binder (wt%)[b]	Moisture level (wt% H_2O)	G.D. (%)[c]	Diameter (μm) Max.[d]	Min.[e]	Amount of deviation (μm)[f]
A/4/V/D	4.7 — PVA	0.0	57.10	10979	10937	42
A/4/V/W	4.7 — PVA	1.2	58.95	10992	10962	30
A/2/V/D	2.4 — PVA	0.0	58.90	11008	10969	39
A/2/V/W	2.4 — PVA	1.2	59.84	11037	11010	27
A/4/G/D	4.7 — PEG	0.0	59.41	11018	10987	31
A/4/G/W	4.7 — PEG	1.3	59.63	11026	11001	25
A/2/G/D	2.4 — PEG	0.0	59.17	10995	10967	28
A/2/G/W	2.4 — PEG	1.1	59.55	11009	10986	23

[a]The properties of the compacts are given in Table 1.
[b]PVA: poly(vinyl alcohol); PEG: poly(ethylene glycol).
[c]The relative green density at a compaction pressure of 370 MPa.
[d]The maximum diameter of the sintered compact.
[e]The minimum diameter of the sintered compact.
[f]The amount of gross deviation = the maximum diameter – the minimum diameter.

Table 5. The data used for the sintering simulation to predict the sintered density

Q_s (Sintering activation energy)	520 kJ/mol
Q_g (Grain growth activation energy)	475 kJ/mol
R (Gas constant)	8.3 J/mol
T (Temperature)	1800 K (1527°C)
n (Grain size exponent)	4
G_o (Initial grain size)	0.4×10^{-6} m
M (Constant)	7.7×10^{-4}
K''' (Grain growth constant)	3.0×10^{-7} m^3/s

same procedure is also used for the prediction of the evolution of the overall shape of these sintered alumina compacts. However, the sintering simulation equations, used in the previous publication, are slightly modified. This procedure may be summarised as follows:

1. (i) The transmission ratios were measured as a function of the aspect ratio.
2. (ii) A first order empirical equation, which describes the inter-relationship between the green density and the compaction pressure, was obtained using low aspect ratio samples.
3. (iii) The density distribution, as a function of the height of the compact, was predicted using the Janssen–Walker analysis [19,20] by incorporating the experimental results obtained in the studies (i) and (ii) described above.
4. (iv) Finally, the overall shapes of the compacts, as a function of the height of the compact, were predicted by using the sintering simulation equations [see eqns (5) and (7)], which inter-relate the final sintered density of the compact to the predicted initial green density distribution.

The data used for these sintering simulations are given in Table 5. The overall shapes of the sintered compacts may then be approximately predicted by using the following equation:

$$D_s(h) = D_o\left(\frac{\bar{\rho}(h)}{\bar{\rho}_s(h)}\right)^{\frac{1}{3}} \tag{9}$$

where $D_s(h)$ is the diameter of the compact at the height h after sintering, D_o is the diameter of the compact before sintering and $\bar{\rho}_s(h)$ is the average computed sintered density of the compact at height h for a given sintering time and temperature. This procedure implicitly assumes a non-affine shrinkage in the sense that radial shrinkages in each orthogonal (with respect to the compaction load axis) plane are confined only to that plane and are also autonomous; that is, each plane of shrinkage is not influenced by its neighbours.

For the prediction of the mean density, along the height of the compacts, the following equation was adopted:[1,3]

$$\bar{\rho}(h) = A + B\ln Q - BC\frac{h}{D} \tag{10}$$

According to eqn (10), the extent of the density distributions in the compacts is dependent upon the magnitude of the product of BC. The density distributions within the compacts, with a greater value of the product BC, will be the most inhomogeneous. As a result, the gross amount of diametrical deviations in those sintered compacts, with the greatest values of the product BC, will be higher. For the soft agglomerates, such as the A/2/G/H, A/2/G/W and A/2/V/W, the densification in the early stages is very efficient; that is, the compacts (prepared using the soft agglomerates) reach quite high green densities at relatively low compaction pressures. In the second stage of the compaction process (usually after the joining pressure), the densification rate of these compacts is not very high since they have already reached quite high densities. Therefore, the value of B for these compacts is lower compared to those systems prepared using the harder agglomerates. As a result, the extent of the shape distortions in the compacts, prepared using the soft agglomerates, is lower than that in the compacts, prepared using the hard agglomerates (see Table 4).

Previously, the overall shape prediction procedure has only been successfully applied for the prediction of the final sintered alumina compacts.[2] In this paper, the progressive overall shape evolution of the sintered alumina compacts (measured and predicted) is reported. The development of the overall shape of the alumina compacts as a function of the sintered density is illustrated in Figs 9

Table 6. The experimental and predicted results for the development of the overall shape of the alumina compacts. (D_P=predicted diameter, D_M=measured diameter)

	ρ_s=93.81		ρ_s=96.02		ρ_s=97.15		ρ_s=98.00		ρ_s=98.47		ρ_s=99.11	
	D_P	D_M	D_P	D_M	D_P	D_M	D_P	D_M	D_P	D_M	D_P	D_M
Maximum D (μm)	11148	11154	11067	11062	11029	11023	10998	11000	10982	10980	10960	10964
Minimum D (μm)	11125	11129	11034	11027	10990	10980	10954	10952	10935	10919	10909	10897
Deviation (μm)	23	25	33	35	39	43	44	48	47	61	51	67

and 10 for the A/2/G/H and M/4.5/G/SD compacts, respectively. As may be seen from these figures, the amount of deviation from the perfect cylindrical geometry increases as the sintered density of the compacts increases.

The sintering kinetics for the A/2/G/H compact system has not been studied. The sintering simulation equations, developed for the A/2.5/V/SD compacts, are used since the same primary alumina particles have been used for the preparation of these agglomerates. This was considered to be a reasonable assumption. The empirical compaction parameters, A, B and C, for the A/2/G/H agglomerates have been determined as 52.07, 1.25 and 0.33, respectively.[3] The density distributions for the A/2/G/V compact ($H/D = 2.11$) may then be calculated using eqn (10). The local maximum and minimum sintered densities of the compacts are determined using the sintering simulation equations and the corresponding diameters of the compact were calculated using eqn (9). The experimental and predicted results for the development of the overall shape of the alumina compacts are summarised in Table 6. As may be seen from Table 6, there is good agreement between the predicted and measured results, in the sense that the shape distortions in the compacts increase with increasing sintered density (Fig. 11).

3.2.5 Near net shape forming of die-pressed compacts

The shape distortions encountered in sintered dry pressed compacts are inevitable due to the inhomogeneous density distributions present in the corresponding green compacts. The inhomogeneous density in the green compacts is the inherent problem associated with the dry die-pressing process, since the applied pressure will not be transmitted uniformly due to the influence of the wall frictional forces. It has already been shown that the shape distortions are considerably reduced with the application of a die wall lubricant and that the optimisation of the agglomerate properties may be optimised in order to reduce the density distributions in the green compacts.

One way to obtain a sintered compact with very small shape distortions is to produce a homogeneous green compact. The corrected green density of the compacts (PVA system) with a low binder content is higher than those of the compacts with

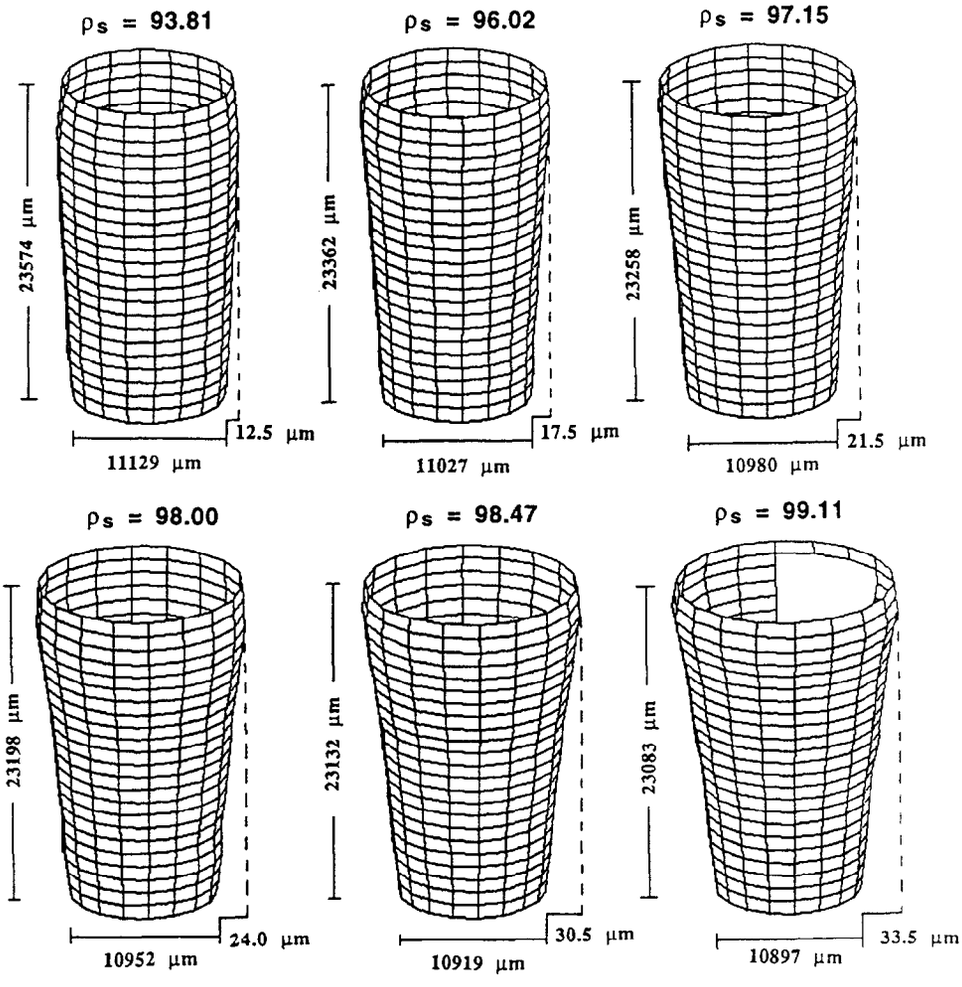

Fig. 9. The development of the overall shape of the A/2/G/H alumina compacts as a function of the sintered density.

a high binder content at the same compaction pressure level. In order to obtain the same green density for these compacts, a lower compaction pressure is required for the compacts with the lower binder content. By taking advantage of the inherent effect in die-pressing — that is, the transmitted pressure is always lower than the applied compaction pressure — it is possible to produce a green compact with a homogeneous density, by creating an appropriate binder content gradient. The procedure for obtaining the proper binder content gradient is illustrated in Fig. 12. The mean compaction pressure, sensed by the slabs, may be calculated using the following equation:

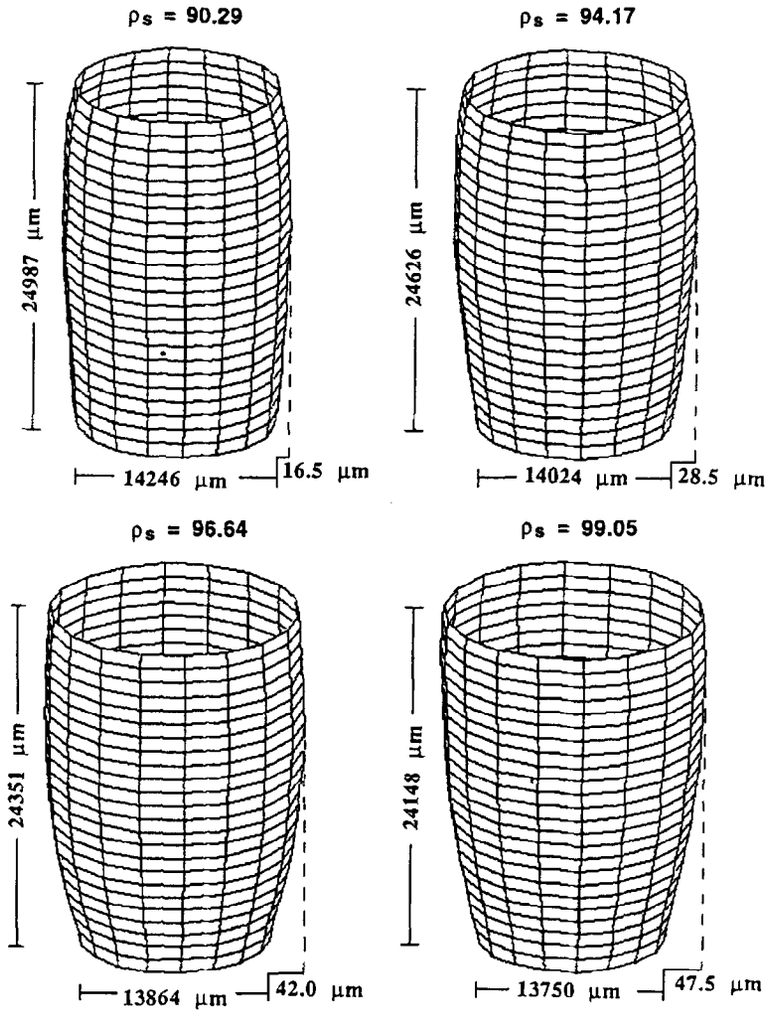

Fig. 10. The development of the overall shape of the M/4.5/G/SD alumina compacts as a function of the sintered density.

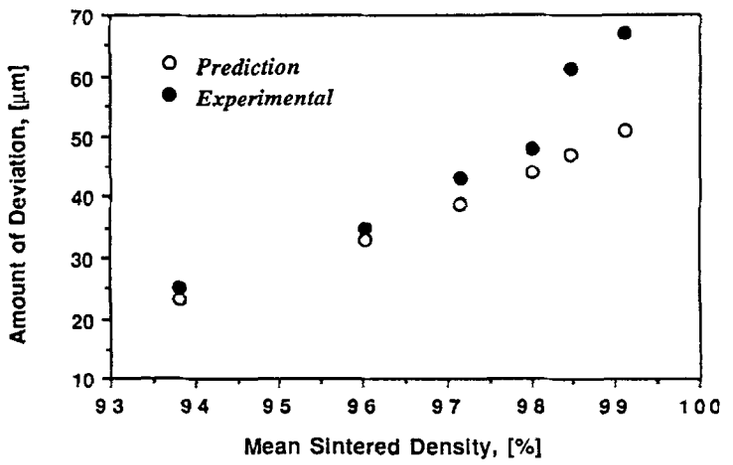

Fig. 11. The amount of diametrical deviation as a function of the mean sintered density for the A/2/G/H compacts.

$$\bar{\sigma}_i = \int_{h_{i-1}}^{h_i} \frac{Q \exp(-C\frac{h}{D})dh}{(h_i - h_{i-1})} \qquad (11)$$

The binder content of the slabs ($b_1 > b_2 > b_3 > b_4 > b_5$) are determined so that the resulting corrected density of the slabs with different mean pressure values can be adjusted to produce the same green density. By using this procedure, the gross amount of deviation from the perfect cylindrical geometry for the alumina compacts, prepared using the agglomerates with various binder (PVA) content, is reduced quite dramatically. Compacts ($H/D = 1.17$) with $\sim 5\,\mu$m diametrical deviation have been successfully produced by this route.

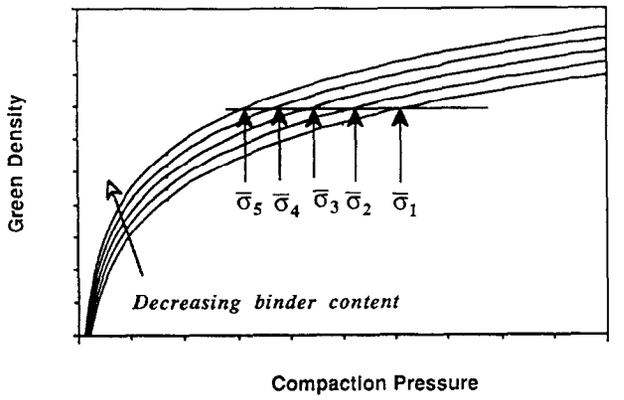

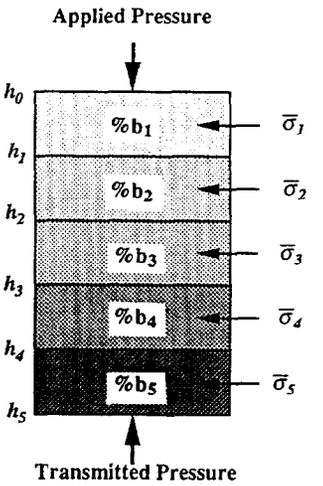

Fig. 12. The schematic representation of the technique for obtaining the appropriate binder content in order to produce a compact with a homogeneous density distribution.

3.2.6 Overall shape of tubes

The overall shapes of tubes, prepared using the uniaxial die-pressing method, were also characterised. The tubes, with a 16.205 mm outer diameter and 9.475 mm inner diameter, were produced using the M/4.5/G/SD and A/2.5/V/SD agglomerates. The overall shapes of the sintered tubes were determined by measuring the outer diameters and also the wall thickness of these tubes. In order to measure the wall thickness of the tubes, the tubes were cut into two pieces in the axial direction. For these tubes, a maximum diameter always exists at the top of the tube. However, it has already been noted that for the simple cylindrical alumina compacts, the maximum diameter existed slightly below the top of the compact. A possible explanation for this contrasting observation is that the density distributions of the tubes, in the lateral direction, are not very significant since the wall thickness of the tubes is not large enough to create any significant density distributions in the lateral direction. This feature can be seen more clearly in Fig. 13, which shows the outer diameter of the compacts ($H/D = 0.57$, 0.87 and 1.16) as a function of the height of the tube. Another interesting feature is that the ratio of the outer diametrical deviation to the wall thickness deviation for the sintered tubes is similar in magnitude to the ratio of the outer diameter to the wall thickness of the

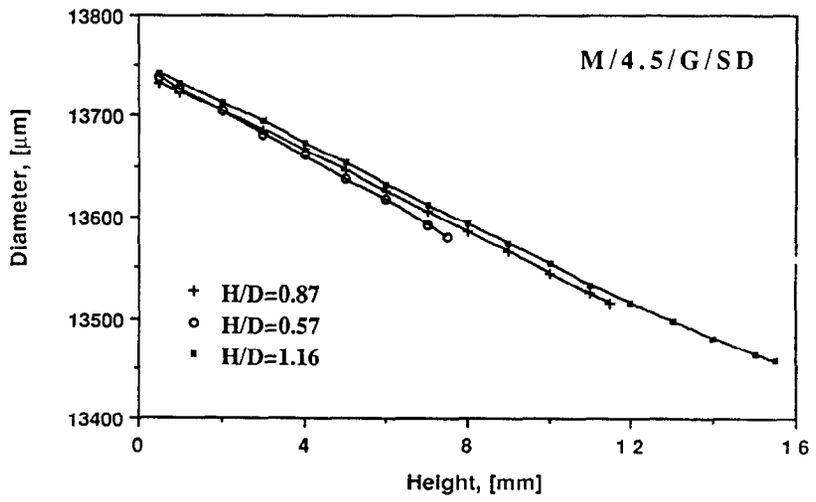

Fig. 13. The outer diameter of the M/4.5/G/SD tubes ($H/D = 0.57$, 0.87 and 1.16) as a function of the height of the tubes.

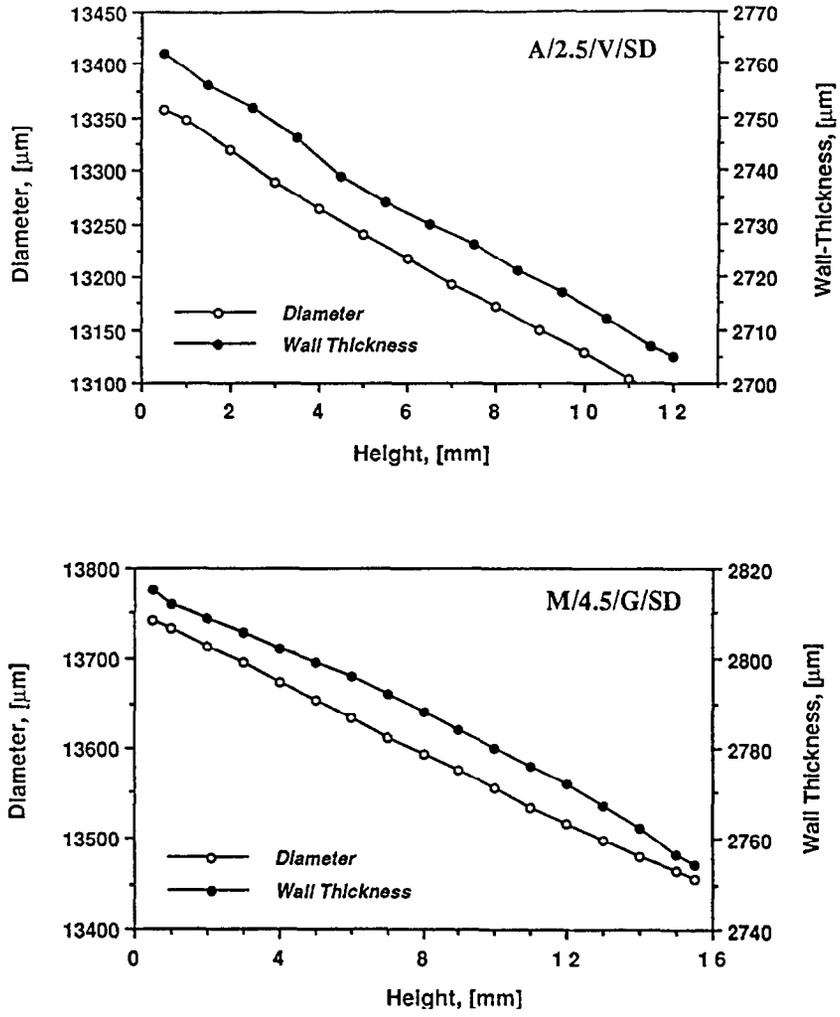

Fig. 14. The outer diameter and the wall thickness of the alumina tubes as a function of the height of the tubes: (a) the A/2.5/V/SD and (b) the M/4.5/G/SD alumina tubes.

green compacts. Figure 14(a) and (b) illustrate the variation of the outer diameter and the wall thickness of the A/2.5/V/SD ($H/D = 0.96$) and M/4.5/G/SD ($H/D = 1.16$) tubes as a function of the height of the tube. The experimental results for these alumina tubes are summarised in Table 7.

4 SUMMARY AND CONCLUSIONS

In general terms, it has been shown that the cylindrical alumina compacts, produced by the uniaxial die-pressing technique, possess a non-uniform green density due to the creation of an uneven stress distribution within the sample, which is controlled in the major part by wall boundary conditions between the compact and the die. It has also been shown that the extent of these density distributions was dependent upon the aspect ratio, the state of die wall lubrication and the properties of the agglomerates. When these compacts with non-homogeneous density distributions are sintered, the shape distortions in the sintered compacts are inevitable since the shrinkage of the regions with different densities in the green compacts is not the same. As a result, the overall shapes of the sintered

Table 7. The experimental results for the alumina tubes

Compact	H/D	Mean ρ_o	Max. OD (μm)	Min. OD (μm)	Max. WT (μm)	Min. WT (μm)	Deviation OD	Deviation WT	Deviation OD/WT
M/4.5/G/SD	0.27	61.43	—	—	—	—	—	—	—
M/4.5/G/SD	0.57	60.72	13739	13581	2814	2782	158	33	4.79
M/4.5/G/SD	0.87	59.72	13733	13515	2818	2773	218	45	4.84
M/4.5/G/SD	1.16	58.99	13743	13456	2815	2754	287	61	4.70
A/2.5/V/SD	0.96	57.11	13358	13081	2762	2704	277	58	4.78
A/2.5/V/SD	1.24	56.79	13322	12979	2747	2675	343	72	4.77

compacts are not geometrically scaled replicas of the green compacts. It has been established that there is an inter-relationship between the shape distortions in the sintered compacts and the density variations in the green compacts; that is, the more inhomogeneous the green compacts the greater is the shape distortion which results in the sintered compacts. Therefore, it is necessary to produce a homogeneous green compact in order to obtain a near net shape final product. It has been shown that the extent of the density distributions in the green compacts have been reduced (i) by optimising the agglomerate properties (the density variations in the compacts prepared using the wet agglomerates is significantly less than that for those compacts prepared using the dry agglomerates), (ii) with the application of an efficient lubricant (zinc stearate) to the die walls, and (iii) by creating an appropriate binder gradient along the height of the compacts. When these relatively homogeneous green compacts have been used, the shape distortions in the corresponding sintered compacts have been significantly reduced. In this study, it has also been shown that by using a simple first order predictive model based on the J–W analysis, combined with a subsidiary compaction equation and a sintering model, the overall shape of the sintered compacts has been predicted accurately.

Specifically, the following conclusions may be inferred.

1. The sintering of the current alumina compacts is found to be generally isotropic for the present systems.
2. The densification rate of the low green density compacts is higher than that for the higher green density compacts. However, the sintered density of the high green density compacts is always higher than that of the low green density compacts. The compacts with low green density shrink more than those with higher density.
3. The interconnected pores, in the alumina compacts, begin to become isolated at around 90% of the theoretical density and all the pores are isolated after 96% of the theoretical density.
4. The gross amount of deviation from the perfect cylindrical geometry for the sintered compacts is the highest for the compacts with the highest aspect ratio.
5. The extent of the shape deviation for the compacts produced in the unlubricated die is much higher than that for the compacts produced in the lubricated die.
6. The agglomerate properties (binder type, binder content and moisture level) affect the overall shape of the sintered alumina compacts. The amount of the deviation for the compacts prepared using the wet agglomerates is significantly less than that for those compacts prepared using the dry agglomerates.
7. The extent of shape distortions of the alumina compacts increases with increasing sintered density.
8. Perhaps the most significant finding, in the manufacturing context, is that by the simple expedient of varying the binder content locally it is possible to engineer near net shape forming of a sintered product to an improved level of precision. Near net shape die-pressed compacts with very small shape distortions (5 μm) have been produced by creating an appropriate binder gradient along the height of the compacts.
9. The values of the outer diameter and the wall thickness of the alumina tubes decrease rather linearly towards the bottom of the tubular systems.

ACKNOWLEDGEMENT

The authors would like to acknowledge the financial support of British Nuclear Fuels plc for the ceramic programme in the particle technology group at Imperial College.

REFERENCES

1. ÖZKAN, N., Compaction and sintering of alumina compacts. Ph.D. Thesis, Imperial College, London, UK, 1994.
2. ÖZKAN, N. & BRISCOE, B. J., Prediction of overall shape of alumina compacts. *J. Eur. Ceram. Soc.*, **14**(20) (1994) 143.
3. ÖZKAN, N. & BRISCOE, B. J., Characterisation of die pressed ceramic compacts. *J. Eur. Ceram. Soc.*, **17** (1997) 697.
4. BRISCOE, B. J., FERNANDO, M. S. D. & SMITH, A. C., The interfacial friction of compacted maize powders. *J. Phys. D: Appl. Phys.*, **18** (1985) 1069.
5. BRISCOE, B. J. & EVANS, P. D., Wall friction in the compaction of agglomerated ceramic powders. *Powder Technol.*, **65** (1991) 7.
6. STEWARD, N. I., Influence of particle size distribution on the sintering of ceramic powder compacts. Ph.D Thesis, Imperial College, London, UK, 1989.
7. OCCHIONERO, M. A. & HALLORAN, J. W., *The Influence of Green Density Upon Sintering, Materials Research Vol. 16*, ed. G. C. Kuczynski, A. E. Miller & G. A. Gordon. Plenum Press, New York, 1984, p. 89.
8. BRUCH, C. A., Sintering kinetics for the high density alumina process. *Am. Ceram. Soc. Bull.*, **41**(12) (1962) 799.
9. RAHAMAN, M. N., DE JONGHE, L. C. & CHU, M.-Y., Effect of green density on densification and creep during sintering. *J. Am. Ceram. Soc.*, **74**(3) (1991) 514.

10. GRESKOVICH, C., Effects of green density on the initial sintering of alumina. *Phys. Sintering*, **4**(1) (1972) 33.
11. WOOLFREY, J. L., Effect of green density on the initial-stage sintering kinetics of UO2. *J. Am. Ceram. Soc.*, **55**(8) (1972) 383.
12. ÖZKAN, N. & BRISCOE, B. J., Effects of green density and consolidation techniques on sintering and microstructure of alumina compacts. In *Proc. Int. Conf. on Materials by Powder Technology*, Dresden, Germany, 23 March 1993, p. 583.
13. ZHAO, J. & HARMER, M. P., Effect of pore distribution on microstructure development — III. Model experiments. *J. Am. Ceram. Soc.*, **75**(4) (1992) 830.
14. BRISCOE, B. J. & ÖZKAN, N., Sintering and microstructural development of alumina compacts. In *Proc. 8th CIMTEC: World Ceramic Congress*, Florence, Italy, July 1994.
15. CAMERON, C. P. & RAJ, R., Grain-growth transition during sintering of colloidally prepared alumina powders. *J. Am. Ceram. Soc.*, **71**(12) (1988) 1031.
16. CARTER, W. C. & GLAESER, A. M., Dihedral angle effects on the stability of pore channels. *J. Am. Ceram. Soc.*, **67**(6) (1984) C124.
17. SWINKELS, F. B. & ASHBY, M. F., Second report on sintering diagrams. *Acta Metall.*, **29** (1981) 259.
18. BRISCOE, B. J. & ÖZKAN, N., Compaction behaviour of agglomerated alumina powders. *Powder Technol.*, in press.
19. JANSSEN, H. A., Versuche uber getreiddruck in silozellen. *Z. Ver. Deutsch. Ing.*, **29** (1895) 1045.
20. WALKER, D. M., An approximate theory for pressures and arching in hoppers. *Chem. Eng. Sci.*, **21** (1966) 275.